Biochimica et Biophysica Acta 1808 (2011) 2496–2500

Contents lists available at ScienceDirect

Biochimica et Biophysica Acta

journal homepage: www.elsevier.com/locate/bbamem

Oxidative stress increases angiotensin receptor type I responsiveness by increasing receptor degree of aggregation using image correlation spectroscopy

Titiwat Sungkaworn [a], Yongwimon Lenbury [b], Varanuj Chatsudthipong [a,*]

[a] Department of Physiology, Faculty of Science, Mahidol University, Bangkok 10400, Thailand
[b] Department of Mathematics, Faculty of Science, Mahidol University and National Centre of Excellence in Mathematics, PERDO, Bangkok 10400, Thailand

ARTICLE INFO

Article history:
Received 2 March 2011
Received in revised form 6 July 2011
Accepted 11 July 2011
Available online 23 July 2011

Keywords:
Oxidative stress
Angiotensin receptor
Image correlation spectroscopy
Aggregation

ABSTRACT

Oxidative stress and hyper-functioning of angiotensin II receptor type I (AT_1R) are commonly observed in hypertensive patients but the relationship between oxidative stress and AT_1R function is still unclear. We investigated the effects of H_2O_2 treatment on AT_1R-mediated intracellular calcium $[Ca^{2+}]_i$ signaling and its cell surface distribution pattern in HEK cells stably expressing EGFP-tagged rat AT_1R using image correlation spectroscopy (ICS). Following H_2O_2 treatment (50–800 μM), $[Ca^{2+}]_i$ was significantly increased upon angiotensin II stimulation. Similarly ICS revealed a significant increase in degree of AT_1R aggregation in H_2O_2 treated group during Ang II activation but no difference in cluster density compared with untreated control cells or those with *N*-acetyl cysteine pretreatment. Thus, oxidative stress-induced AT_1R hyper-responsiveness can be attributed by an increase in cell surface receptor aggregation state, possibly stemming in part from oxidant-related increase receptor–receptor interactions.

1. Introduction

Angiotensin II receptor is a G-protein coupled receptor (GPCR) for vasoactive peptide angiotensin II (Ang II) in the renin-angiotensin system (RAS), which plays a crucial role in the control of body water-electrolyte balance and in blood pressure regulation [1]. Two subtypes of Ang II receptor have been characterized, namely, angiotensin II receptor type I (AT_1R) and type II (AT_2R), with the former playing a predominant function in mediating various physiological functions [2]. Human [3] and rat [4,5] AT_1R have been cloned, and based on homology comparison, AT_1R belongs to family A of GPCR superfamily [2]. Upon stimulation by Ang II, $G_{q/11}$ - phospholipase C-inositol triphosphate (IP3) pathway is activated leading to an increase in intracellular calcium level. Subsequently, downstream proteins are activated generating a variety of cellular responses, such as vasoconstriction, increased renal Na^+ reabsorption and aldosterone secretion, all of which ultimately control body water balance and blood pressure [6].

Abnormality of AT_1R signaling can lead to the development of pathological conditions, especially those involving cardiovascular diseases, such as hypertension and atherosclerosis [7]. Hyper-function of AT_1R is commonly observed in hypertension, and thus, AT_1R modulators/antagonists are of potential utility for the treatment of hypertension. Selective AT_1R antagonists, such as losartan, valsartan and candesartan, are in current use as the drugs for hypertensive patient [8]. However, the mechanism by which AT_1R signaling contributes to hypertension remains unclear. Reactive oxygen species (ROS), the product from oxidative stress, was found to play crucial roles in pathological conditions of cardiovascular system [9,10]. Recently, Banday et al. [11,12] have shown that AT_1R content was upregulated at both mRNA and protein levels in oxidant (L-buthionine sulfoximine)-treated rat, resulting in abnormally high blood pressure. Both AT_1R upregulation and hypertension in oxidant-treated rat were abolished by antioxidant, tempol, administration. This evidence clearly shows an interplay between oxidative stress and AT_1R signaling in the development of hypertension. Oxidative stress has also been shown to affect the distribution pattern of mature AT_1R on cell membrane [13]. H_2O_2 induces AT_1R dimer formation, based on Western blotting analysis, in human embryonic kidney (HEK) cells stably expressing AT_1R [13]. Moreover, in monocytes from hypertensive patients, AT_1R is present in a dimeric form, resulting in hyper-responsiveness of AT_1R to Ang II which contributes to the initial state of atherosclerosis [14]. However, the role of oxidative stress on AT_1R distribution pattern and function in intact cell membrane has not yet been studied.

A recent technique used to quantitatively analyze distribution patterns of membrane proteins, especially membrane receptors, is image correlation spectroscopy (ICS) [15,16]. Although ICS has a

Abbreviations: AT_1R, angiotensin II receptor type I; AT_2R, angiotensin II receptor type II; Ang II, angiotensin II; BMP, bone morphogenetic protein; CD, cluster density; DA, degree of aggregation; EGFP, enhanced green fluorescent protein; GPCR, G - protein coupled receptor; HBSS, Hanks' balanced salt solution; HEK cell, human embryonic kidney cell; ICS, image correlation spectroscopy; IP3, inositol triphosphate; $[Ca^{2+}]_i$, intracellular calcium concentration; MTT, thiazolyl blue tetrazolium bromide; NAC, *N*-acetyl cysteine; NOX1, NADPH oxidase 1; RAS, renin angiotensin system; ROS, reactive oxygen species

* Corresponding author at: Department of Physiology, Faculty of Science, Mahidol University, Rama 6 Road, Bangkok 10400, Thailand. Tel.: +66 2 201 5614; fax: +66 2 354 7154.
E-mail address: scvcs@mahidol.ac.th (V. Chatsudthipong).

0005-2736/$ – see front matter © 2011 Elsevier B.V. All rights reserved.
doi:10.1016/j.bbamem.2011.07.007

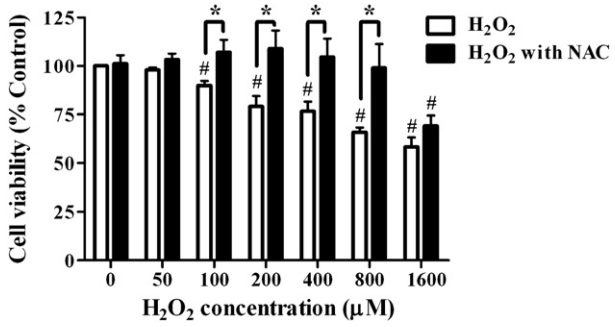

Fig. 1. Effect of H_2O_2 treatment on AT_1R-HEK cell viability. Confluent AT_1R–HEK cells were exposed to H_2O_2 at the indicated concentrations for 3 h and assayed for viability using MTT method. Controls included untreated cells and those prior treated with 4 mM *N*-acetyl cysteine (NAC) for 24 h. * $p<0.05$ compared with NAC-treated groups, and # $p<0.05$ compared with control group, n = 4–10.

limitation for examining biochemical interaction at single molecule level, it does allow examination of the distribution pattern of proteins in native membrane, in which protein conformation, protein–protein interaction and membrane lipids are not perturbed. Thus, ICS provides a good approach to investigate membrane receptor distribution patterns in native cells. For example, Nohe et al. [17] used this technique to demonstrate that bone morphogenetic protein (BMP) receptor rearrangement following its cognate ligand binding is essential for activation of BMP receptor and Smad pathway. Similarly, ligand-induced receptor clustering was also observed for epidermal growth factor [18] and platelet-derived growth factor [19] receptors in order to obtain effective trans-membrane signaling.

In this study, we investigated the effect of oxidative stress on cell-surface AT_1R distribution pattern using microscopic approach with image processing technique (ICS). In addition, the effect of H_2O_2 treatment on AT_1R-mediated intracellular calcium signaling was examined.

2. Materials and methods

2.1. Cell culture

Human embryonic kidney cells (HEK293) stably expressing EGFP-tagged rat AT_1R (AT_1R–HEK cells) were kindly provided by Dr.Tamás Balla, National Institutes of Health, USA [20]. AT_1R used for transfection was $AT_{1a}R$ subtype. AT_1R–HEK cells were cultured in Dulbecco's modified Eagle medium (Invitrogen), supplemented with 10% heat-inactivated fetal bovine serum (HyClone), 100 U/ml penicillin and 100 μg/ml streptomycin (Invitrogen), at 37 °C in a humidified atmosphere of 5% CO_2. The selection for maintaining EGFP-tagged AT_1R expression was performed every two weeks using medium containing 500 μg/ml Geniticin (Invitrogen).

2.2. Oxidant treatment and cell viability assay

AT_1R–HEK cells were seeded in 96-well plate at a density of 2×10^4 cell/well. Confluent cells were exposed to H_2O_2 (50 to 1600 μM) as oxidant treatment for 3 h at 37 °C in a humidified atmosphere of 5% CO_2. Pre-incubation overnight with 4 mM *N*-acetyl cysteine (NAC) alone was also included as antioxidant control. Then, cell viability was determined using MTT assay [21].

2.3. Intracellular calcium measurement

A fluorometric-based assay was used to determine intracellular calcium level. Confluent AT_1R–HEK cells were trypsinized and washed twice with Hanks' balanced salt solution (HBSS). Then, they were resuspended to obtain a density of 2×10^6 cell/mL and incubated with 6 μg/mL indo1-AM (Invitrogen) at 37 °C for 60 min. Subsequently, cells were washed twice with Ca^{2+} flux buffer (HBSS supplemented with 1% bovine serum albumin (Calbiochem) and 1 mM $CaCl_2$) and resuspended in Ca^{2+} flux buffer to a density of 1×10^6 cell/mL. Intracellular calcium level of un-stimulated baseline and upon Ang II stimulation was measured as a ratio of fluorescent emission (R) at 405 nm and 490 nm, excitation wavelength of 338 nm, using the following formula [22]:

$$\left[Ca^{2+}\right]_i = K_d\left[\frac{(R-R_{\min})}{(R_{\max}-R)}\right]\left[\frac{S_{f2}}{S_{b2}}\right] \quad (1)$$

where K_d is the dissociation constant of indo1-AM and (S_{f2}/S_{b2}) is the fluorescence ratio of emission wavelength at 490 nm in the absence of Ca^{2+} (3 mM of EGTA) to that at Ca^{2+} saturation (5 μM of ionomycin (Calbiochem)). Calcium level upon Ang II stimulation was obtained from the peak of fluorescent signal after Ang II administration.

2.4. Image correlation spectroscopy(ICS) and image processing

EGFP-tagged AT_1R-HEK cells were placed in cover glass bottom black dish (Electron Microscopy Sciences) at a density of 1.5×10^5 cell/plate and visualized using a 488 nm laser line under a 60× oil immersion objective. The image was captured with a 3× digital zoom at a pixel resolution of 0.1 μm/pixel (Olympus, FLUOVIEW® FV1000). Z–stack capture mode was applied at 0.5 μm height for each step. The final image was composed of 30–40 individual planar cross-section images, which were reconstructed to reveal surface receptor distribution. The images, which were captured before and after 1.0 nM Ang II treatment, were processed by ICS [15] to determine receptor distribution parameters,

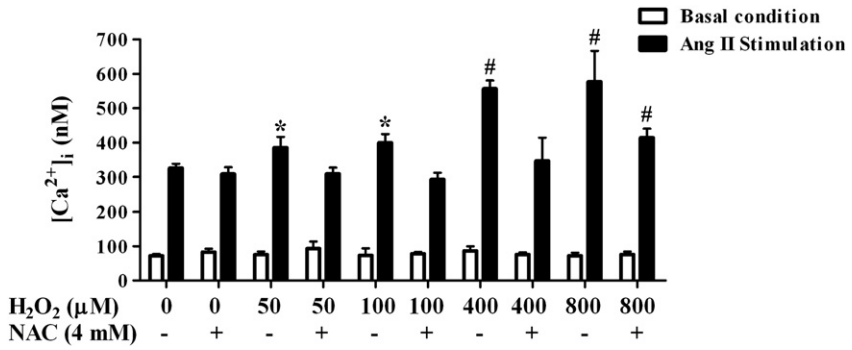

Fig. 2. Effect of H_2O_2 treatment on angiotensin signaling of AT_1R-HEK cells. Confluent AT_1R–HEK cells were exposed to H_2O_2 at the indicated concentrations for 3 h. The basal intracellular Ca^{2+}, $[Ca^{2+}]_i$, and $[Ca^{2+}]_i$ following Ang II stimulation were determined using a fluorometric method. * $p<0.05$ and # $p<0.01$ compared with control group (AngII treatment alone), n = 3–12.

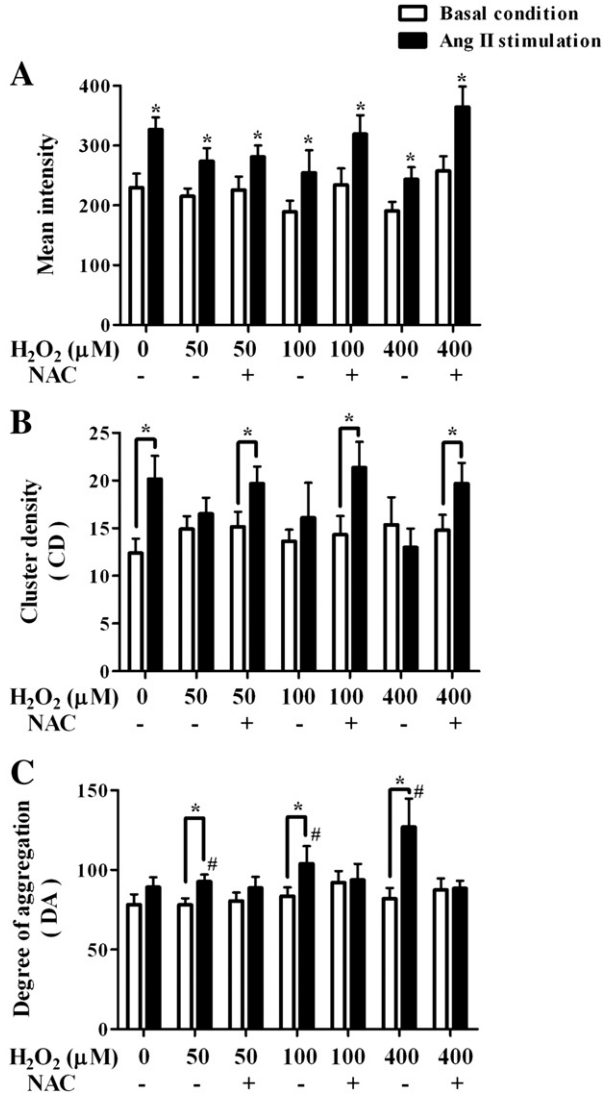

Fig. 3. Effect of angiotensin II on mean fluorescence intensity, cluster density and degree of aggregation of cell surface EGFP-tagged AT_1R of HEK cells. Cells were treated with various doses of H_2O_2 for 3 h prior to image capture under confocal microscope with a 60× oil immersion objective, and NAC was used as indicated to prevent H_2O_2-induced oxidative stress. The image was captured with Z-stack capture mode applied at 0.5 μm height for each step. The final image was composed of 30–40 individual planar cross-section images, which were reconstructed to reveal surface receptor distribution. The images, which were captured before and after 1.0 nM Ang II treatment, were processed by ICS to determine receptor distribution parameters. A. Mean fluorescence intensity of cell surface EGFP-tagged AT_1R was measured. * $p<0.05$ compared with non-AngII stimulated (basal) group at each condition, n = 11–60. B. Cluster density. CD was calculated from the confocal image of EGFP-tagged AT_1R–HEK cells using ICS. In control and H_2O_2 with NAC treated group, Ang II stimulation caused a significant increase in CD. Whereas, there was no change in CD of H_2O_2-treated group at all doses when compared between absence and presence of Ang II. * $p<0.05$ compared with non-AngII stimulated (basal) group at each condition, n = 11–60. C. Degree of aggregation. DA was examined by ICS. Ang II stimulation did not change DA of EGFP-tagged AT_1R in all control and H_2O_2 with NAC treated groups. However, in H_2O_2-treated group, DA was significantly increased in the presence of Ang II stimulation. * $p<0.05$ compared with non-AngII stimulated (basal) group at each condition, # $p<0.05$ compared with control group, n = 11–60.

namely, cluster density (CD) and degree of aggregation (DA). Image acquisition and region selection criteria were followed as previously reported [23]. The criteria were as follows. (a) High noise and saturated fluorescent images were excluded. (b) Images for ICS analysis did not have a pixel size larger than 0.1 μm/pixel. (c) Images of interface regions between two cells or edges of a cell were avoided. d) Regions analyzed with ICS were entirely on the cell surface. Spatial correlation function, g(x,y), was determined as described previously [16,24]. Then, the correlation function was fitted to a two-dimensional Gaussian function (Eq. (2)).

$$g(x,y) = g(0,0)e^{-(x^2+y^2)/\omega^2} + g_0 \quad (2)$$

where g(x,y) is the spatial correlation function of position coordinate x and y, ω represents the laser beam width, and g(0,0) is the amplitude of the correlation function at the origin.

The average number of independent fluorescent particles per laser beam area ($\overline{N}_p$), which is equal to the inverse of g(0,0) [18], was normalized to the laser beam area in order to obtain CD value (Eq. (3)).

$$CD = \frac{1}{g(0,0)\pi\omega^2} \quad (3)$$

DA is defined as the average number of fluorescent molecules ($\overline{N}_m$) in the protein cluster. DA was determined from the ratio of $\overline{N}_m$, which is proportional to the mean fluorescent intensity (i(x,y)), to the average number of independent fluorescent particles, ($\overline{N}_p$). Then, DA was calculated using Eq. (4).

$$DA = \langle i(x,y)g(0,0)\rangle = c\frac{\overline{N}_m}{\overline{N}_p} \quad (4)$$

where c is a constant value governed by the imaging system efficiency and was not determined in this experiment, thus all DA value are presented as relative values.

2.5. Statistical analysis

Student's *t*-test and one-way ANOVA with Tukey post hoc test were used to analyze experimental data. Significant difference was determined at $p<0.05$. All experimental results are expressed as mean ± S.E. from at least three independent experiments conducted in triplicate.

3. Results

3.1. Effect of oxidative stress on cell viability

To mimic the pathological condition of oxidative stress, AT_1R-HEK cells were treated with H_2O_2 at various concentrations (50–1600 μM) for 3 h and then cell viability was examined using MTT assay. NAC, an anti-oxidant compound, was used to prevent oxidative stress as NAC can directly and specifically react with several ROS including H_2O_2, and it is the precursor in the glutathione biosynthetic pathway, which will increase the intracellular level of this free radical scavenger [25,26]. The results showed that H_2O_2 decreased cell viability in a dose-dependent manner from a minimum of 100 μM H_2O_2 ($p<0.05$) (Fig. 1). The cytotoxic effect of H_2O_2 (up to 800 μM) was completely prevented by preincubating the cells overnight with 4 mM NAC.

3.2. Effect of oxidative stress on angiotensin signaling

To investigate whether oxidative stress can modulate AT_1R function, the response of AT_1R to its native ligand, Ang II (1.0 nM), was determined by measuring intracellular Ca^{2+} concentration, which reflects the activation of AT_1R signaling pathway. Ang II-induced elevation of intracellular Ca^{2+} level is significantly increased in AT_1R-HEK cells treated with 50 μM, 100 μM, 400 μM and 800 μM H_2O_2 compared to non-oxidative stressed control cells ($p<0.05$)(Fig. 2). This hyper-responsiveness to Ang II stimulation of oxidant-stressed cells was abolished by NAC pretreatment.

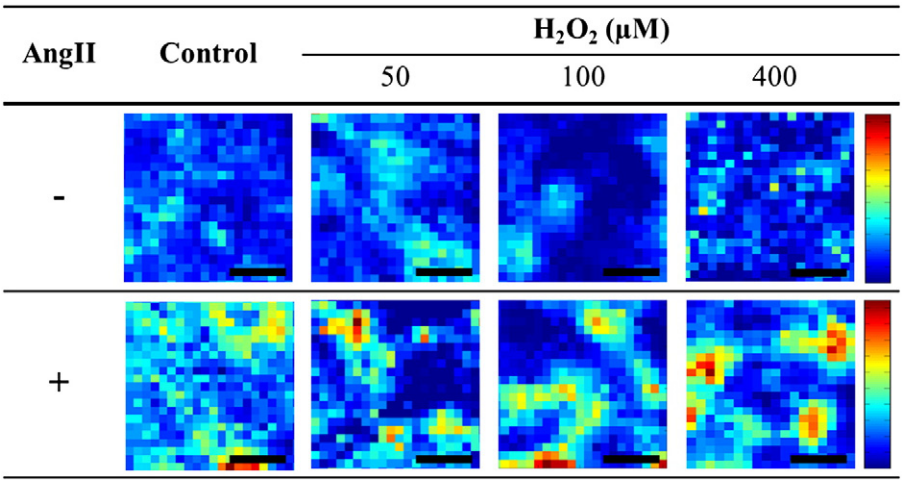

Fig. 4. Effect of H_2O_2 treatment on cell membrane AT_1R distribution pattern. The fluorescent intensity image reveals AT_1R distribution on cell membrane. Colored scale bar on the right indicates fluorescent intensity ranging from low (blue) to high intensity (red). Ang II stimulation increased the presence of AT_1R on cell membrane in all groups. However, Ang II-induced AT_1R aggregation, which is represented by cluster of orange-red color, was found only in H_2O_2-treated group. Indicated scale bar represents 1 μm.

3.3. Cell-surface AT_1R distribution pattern in oxidant-stressed cells

Recently, the distribution pattern of receptors on cell surface has been proposed as being an important factor for determining receptor function [15,27]. In this study, cell-surface AT_1R distribution pattern of intact cells was investigated using ICS, which allows mean fluorescence intensity, CD and DA of cell-surface AT_1R to be analyzed [15,16,24].

The numbers of AT_1R on cell membrane upon stimulation with 1.0 nM Ang II are significantly elevated in all groups (control, H_2O_2 treatment, and H_2O_2 with NAC treatment) ($p<0.05$) as indicated by the increase in mean fluorescence intensity of EGFP–tagged AT_1R (Fig. 3A). Ang II treatment of AT_1R-HEK cells resulted in significant increase in CD values, representing the numbers of independent particles ($\overline{N}_p$) or clusters per area of cell membrane, of control and H_2O_2 with NAC treated groups ($p<0.05$) (Fig. 3B). This result correlated with the changes in mean intensity of EGFP-tagged AT_1R.

Interestingly, there were no changes in CD of H_2O_2-treated cells following Ang II stimulation, although there were increases in mean fluorescence intensity. To further understand this phenomenon, DA, which represents the number of molecules in each protein cluster and thus reflects the size of receptor cluster, was calculated. In the presence of Ang II, DA of H_2O_2-treated cells was significantly increased ($p<0.05$) with tendency to be dose responsive (Fig. 3C). However, this increase in DA was not observed in both control and all doses of H_2O_2 with NAC-treated groups.

In short, Ang II stimulation caused an increase in AT_1R numbers on cell membrane. These higher amounts of membrane AT_1R caused an increase in numbers of receptor CD in control and H_2O_2 with NAC-treated cells, whereas, in H_2O_2-treated cells, the increase in membrane AT_1R caused by Ang II stimulation did not change CD, but caused an increase in size of cluster as observed from the increase in DA (Fig. 4). This reflects H_2O_2-induced AT_1R aggregation/clustering upon receptor activation.

4. Discussion

We demonstrated an alteration of AT_1R function and cell membrane distribution pattern of AT_1R–HEK cells under H_2O_2-induced oxidative stress. H_2O_2 treatment of 50–800 μM promoted hyper-responsiveness of AT_1R to Ang II stimulation as manifested by elevation in intracellular calcium concentration. In addition, a ligand-dependent change in cell surface distribution pattern of AT_1R to favor an aggregation state was shown by an increase in DA without any change in CD.

AT_1R is a key player in the RAS system, which regulates blood pressure and body fluid homeostasis. Alteration of AT_1R function contributes to several pathological conditions, especially of the cardiovascular system [7]. Oxidative stress is commonly observed in hypertension, atherosclerosis, cardiac hypertrophy and heart failure [28]. In spontaneous hypertensive rat, H_2O_2 treatment induces AT_1R hyper-responsiveness and enhances AT_1R content in cell membrane lipid raft [29], data which are consistent with our findings in HEK cell line.

Changes in distribution patterns of cell surface receptors have been proposed as a novel determining factor for modulating receptor function [18,27]. ICS allows cell surface AT_1R distribution pattern to be examined via three parameters, which are mean fluorescent intensity that reflects cell surface content, CD indicating the average number of independent particles or clusters per unit of surface area, and DA, indicative of cluster size [17–19].

Our results showed that in AT_1R–HEK cells, Ang II induced a higher presence of cell surface AT_1R, even in oxidative stress cells. Agonist-induced receptor insertion is a rare event for GPCRs, although this phenomenon is seen with delta opioid receptor when stimulated with its selective agonist, deltorphin-I within 5 min [30]. An alternative explanation is an agonist-induced reduction in surface receptor internalization, i.e. Kinin B_1 receptor, a member of GPCR superfamily, is translocated to caveolae-related raft on cell membrane after receptor activation and thereafter does not undergo internalization [31]. Similarly, upon Ang II stimulation, AT_1R is rapidly translocated to caveolae-related raft [32], which may have resulted in a down-regulation of receptor internalization.

Increase in cell surface protein mean density should be reflected in a concomitant rise in CD value, which is observed for all groups of AT_1R-HEK cells treated with Ang II, except in the case of H_2O_2 treatment, where there were no changes in CD values. However, in the latter situation an increase in DA was observed instead. Ang II-induced increasing DA in H_2O_2 treated group implies that when AT_1R was activated, its distribution pattern on cell membrane was altered to favor an aggregation state under oxidative stress. Agonist-induced membrane receptor rearrangement also occurred in many GPCRs such as chemokine receptor CCR5, delta-opioid receptor, kinin B_1 receptor and thyrotropin-releasing hormone receptor [31,33–35]. The agonist-induced receptor–receptor interaction of these receptors on cell

membrane was proposed as an essential event to establish their function in physiological condition. However, the alteration of cell surface AT_1R arrangement was also involved in its hyper-function during pathological condition.

Cell surface AT_1R exists in a dimeric form in monocytes of hypertensive patients, who have hyper-responsiveness to Ang II stimulation and increased adhesion of monocytes to vascular endothelium during onset of arthrosclerosis [14]. H_2O_2 has been shown to induce AT_1R homodimer formation in AT_1R–HEK cells [13]. Thus, the H_2O_2-induced increase in DA of cell surface AT_1R may be attributed to clusters formed by such AT_1R dimers, thereby resulting in the observed hyper-responsiveness to Ang II stimulation. Although the mechanism by which H_2O_2 causes AT_1R dimer formation is unclear, ROS has been reported to directly cross-link AT_2R to form a dimer in the hippocampus of Alzheimer disease-like mouse [36]. Recently, Basset et al. [37] demonstrated that in aortic smooth muscle from NADPH oxidase 1 (NOX1)-deficient mice, which have abnormally low ROS production, there is a marked decrease in Ang II-induced Ca^{2+} signaling. In addition, NOX1-derived ROS has been proposed to regulate AT_1R targeting and its cell surface expression level [37].

In summary, using ICS, we could elucidate changes in cell surface EGFP-tagged AT_1R density and its distribution pattern. Under oxidative stress condition there was hyper-responsiveness to Ang II stimulation, which was attributed to an increase in AT_1R cell surface aggregation state, possibly caused by oxidant-induced receptor dimerization. Thus, our findings demonstrate the crucial role of cell-surface AT_1R distribution pattern on signal transduction in intact cell membrane. This may provide a basis for development of novel therapeutic approach by modulating AT_1R distribution patterns in certain pathological conditions such as hypertension and atherosclerosis.

Acknowledgements

We gratefully acknowledge Prof. Prapon Wilairat for valuable comments on the manuscript, Dr.Tamás Balla for kindly providing the cell model used in all experiments, and Dr.Paisan Kanthang for helpful suggestions in image processing technique. This work was supported by the Thailand Research Fund through the Royal Golden Jubilee Ph.D. Program (Grant PHD/0245/2548 to T.S. and V.C.), the National Center for Genetic Engineering and Biotechnology (BIOTEC), National Science and Technology Development Agency (NSTDA, Thailand) (Grant 3-2548 to V.C.) and the Office of the Higher Education Commission and Mahidol University under the National Research Universities Initiative (Grant to V.C.).

References

[1] T. Matsusaka, I. Ichikawa, Biological functions of angiotensin and its receptors, Annu. Rev. Physiol. 59 (1997) 395–412.
[2] M. de Gasparo, K.J. Catt, T. Inagami, J.W. Wright, T. Unger, International union of pharmacology. XXIII. The angiotensin II receptors, Pharmacol. Rev. 52 (2000) 415–472.
[3] R. Takayanagi, K. Ohnaka, Y. Sakai, R. Nakao, T. Yanase, M. Haji, T. Inagami, H. Furuta, D.F. Gou, M. Nakamuta, et al., Molecular cloning, sequence analysis and expression of a cDNA encoding human type-1 angiotensin II receptor, Biochem. Biophys. Res. Commun. 183 (1992) 910–916.
[4] T.J. Murphy, R.W. Alexander, K.K. Griendling, M.S. Runge, K.E. Bernstein, Isolation of a cDNA encoding the vascular type-1 angiotensin II receptor, Nature 351 (1991) 233–236.
[5] K. Sasaki, Y. Yamano, S. Bardhan, N. Iwai, J.J. Murray, M. Hasegawa, Y. Matsuda, T. Inagami, Cloning and expression of a complementary DNA encoding a bovine adrenal angiotensin II type-1 receptor, Nature 351 (1991) 230–233.
[6] C. Oro, H. Qian, W.G. Thomas, Type 1 angiotensin receptor pharmacology: signaling beyond G proteins, Pharmacol. Ther. 113 (2007) 210–226.
[7] P.K. Mehta, K.K. Griendling, Angiotensin II cell signaling: physiological and pathological effects in the cardiovascular system, Am. J. Physiol. Cell Physiol. 292 (2007) C82–C97.
[8] M. Burnier, Angiotensin II type 1 receptor blockers, Circulation 103 (2001) 904–912.
[9] K.K. Griendling, D. Sorescu, M. Ushio-Fukai, NAD(P)H oxidase: role in cardiovascular biology and disease, Circ. Res. 86 (2000) 494–501.
[10] H. Ohtsu, G.D. Frank, H. Utsunomiya, S. Eguchi, Redox-dependent protein kinase regulation by angiotensin II: mechanistic insights and its pathophysiology, Antioxid. Redox Signal. 7 (2005) 1315–1326.
[11] A.A. Banday, M.F. Lokhandwala, Oxidative stress-induced renal angiotensin AT1 receptor upregulation causes increased stimulation of sodium transporters and hypertension, Am. J. Physiol. Renal Physiol. 295 (2008) F698–F706.
[12] A.A. Banday, A.B. Muhammad, F.R. Fazili, M. Lokhandwala, Mechanisms of oxidative stress-induced increase in salt sensitivity and development of hypertension in Sprague–Dawley rats, Hypertension 49 (2007) 664–671.
[13] S. AbdAlla, H. Lother, A. el Massiery, U. Quitterer, Increased AT(1) receptor heterodimers in preeclampsia mediate enhanced angiotensin II responsiveness, Nat. Med. 7 (2001) 1003–1009.
[14] S. AbdAlla, H. Lother, A. Langer, Y. el Faramawy, U. Quitterer, Factor XIIIA transglutaminase crosslinks AT1 receptor dimers of monocytes at the onset of atherosclerosis, Cell 119 (2004) 343–354.
[15] A. Nohe, N.O. Petersen, Image correlation spectroscopy, Sci. STKE 2007 (2007) l7.
[16] N.O. Petersen, P.L. Hoddelius, P.W. Wiseman, O. Seger, K.E. Magnusson, Quantitation of membrane receptor distributions by image correlation spectroscopy: concept and application, Biophys. J. 65 (1993) 1135–1146.
[17] A. Nohe, E. Keating, T.M. Underhill, P. Knaus, N.O. Petersen, Effect of the distribution and clustering of the type I A BMP receptor (ALK3) with the type II BMP receptor on the activation of signalling pathways, J. Cell Sci. 116 (2003) 3277–3284.
[18] E. Keating, A. Nohe, N.O. Petersen, Studies of distribution, location and dynamic properties of EGFR on the cell surface measured by image correlation spectroscopy, Eur. Biophys. J. 37 (2008) 469–481.
[19] P.W. Wiseman, P. Hoddelius, N.O. Petersen, K.E. Magnusson, Aggregation of PDGF-beta receptors in human skin fibroblasts: characterization by image correlation spectroscopy (ICS), FEBS Lett. 401 (1997) 43–48.
[20] L. Hunyady, A.J. Baukal, Z. Gaborik, J.A. Olivares-Reyes, M. Bor, M. Szaszak, R. Lodge, K.J. Catt, T. Balla, Differential PI 3-kinase dependence of early and late phases of recycling of the internalized AT1 angiotensin receptor, J. Cell Biol. 157 (2002) 1211–1222.
[21] J. Carmichael, W.G. DeGraff, A.F. Gazdar, J.D. Minna, J.B. Mitchell, Evaluation of a tetrazolium-based semiautomated colorimetric assay: assessment of chemosensitivity testing, Cancer Res. 47 (1987) 936–942.
[22] A. Nelemans, Measurement of [Ca2+] in cell suspensions using indo-1, Methods Mol. Biol. 312 (2006) 47–53.
[23] D.L. Kolin, P.W. Wiseman, Advances in image correlation spectroscopy: measuring number densities, aggregation states, and dynamics of fluorescently labeled macromolecules in cells, Cell Biochem. Biophys. 49 (2007) 141–164.
[24] P.W. Wiseman, N.O. Petersen, Image correlation spectroscopy. II. Optimization for ultrasensitive detection of preexisting platelet-derived growth factor-beta receptor oligomers on intact cells, Biophys. J. 76 (1999) 963–977.
[25] O.I. Aruoma, B. Halliwell, B.M. Hoey, J. Butler, The antioxidant action of N-acetylcysteine: its reaction with hydrogen peroxide, hydroxyl radical, superoxide, and hypochlorous acid, Free Radic. Biol. Med. 6 (1989) 593–597.
[26] A. Gillissen, D. Nowak, Characterization of N-acetylcysteine and ambroxol in anti-oxidant therapy, Respir. Med. 92 (1998) 609–623.
[27] A.H. Clayton, F. Walker, S.G. Orchard, C. Henderson, D. Fuchs, J. Rothacker, E.C. Nice, A. W. Burgess, Ligand-induced dimer-tetramer transition during the activation of the cell surface epidermal growth factor receptor-A multidimensional microscopy analysis, J. Biol. Chem. 280 (2005) 30392–30399.
[28] P.L. Huang, eNOS, metabolic syndrome and cardiovascular disease, Trends Endocrinol. Metab. 20 (2009) 295–302.
[29] R. Pedrosa, V.A. Villar, A.M. Pascua, S. Simao, U. Hopfer, P.A. Jose, P. Soares-da-Silva, H2O2 stimulation of the Cl-/HCO3-exchanger by angiotensin II and angiotensin II type 1 receptor distribution in membrane microdomains, Hypertension 51 (2008) 1332–1338.
[30] L. Bao, S.X. Jin, C. Zhang, L.H. Wang, Z.Z. Xu, F.X. Zhang, L.C. Wang, F.S. Ning, H.J. Cai, J.S. Guan, H.S. Xiao, Z.Q. Xu, C. He, T. Hokfelt, Z. Zhou, X. Zhang, Activation of delta opioid receptors induces receptor insertion and neuropeptide secretion, Neuron 37 (2003) 121–133.
[31] T. Sabourin, L. Bastien, D.R. Bachvarov, F. Marceau, Agonist-induced translocation of the kinin B(1) receptor to caveolae-related rafts, Mol. Pharmacol. 61 (2002) 546–553.
[32] N. Ishizaka, K.K. Griendling, B. Lassegue, R.W. Alexander, Angiotensin II type 1 receptor: relationship with caveolae and caveolin after initial agonist stimulation, Hypertension 32 (1998) 459–466.
[33] S. Cvejic, L.A. Devi, Dimerization of the delta opioid receptor: implication for a role in receptor internalization, J. Biol. Chem. 272 (1997) 26959–26964.
[34] K.M. Kroeger, A.C. Hanyaloglu, R.M. Seeber, L.E. Miles, K.A. Eidne, Constitutive and agonist-dependent homo-oligomerization of the thyrotropin-releasing hormone receptor. Detection in living cells using bioluminescence resonance energy transfer, J. Biol. Chem. 276 (2001) 12736–12743.
[35] A.J. Vila-Coro, M. Mellado, A. Martin de Ana, P. Lucas, G. del Real, A.C. Martinez, J.M. Rodriguez-Frade, HIV-1 infection through the CCR5 receptor is blocked by receptor dimerization, Proc. Natl. Acad. Sci. U.S.A. 97 (2000) 3388–3393.
[36] S. AbdAlla, H. Lother, A. el Missiry, A. Langer, P. Sergeev, Y. el Faramawy, U. Quitterer, Angiotensin II AT2 receptor oligomers mediate G-protein dysfunction in an animal model of Alzheimer disease, J. Biol. Chem. 284 (2009) 6554–6565.
[37] O. Basset, C. Deffert, M. Foti, K. Bedard, V. Jaquet, E. Ogier-Denis, K.H. Krause, NADPH oxidase 1 deficiency alters caveolin phosphorylation and angiotensin II-receptor localization in vascular smooth muscle, Antioxid. Redox Signal. 11 (2009) 2371–2384.